International Journal of Transportation Engineering and Traffic System
ISSN-2456-2343 (online)
Vol. 1: Issue 1
www.journalspub.com

Implementation of Close Range Photogrammetry to Evaluate Distresses at Asphalt Pavement Surface

Saad Issa Sarsam*, Afrah Mekki Daham, Amal Mahdi Ali
Department of Civil Engineering, College of Engineering, University of Baghdad, Baghdad, Iraq

Abstract
Roadway pavements surface deteriorate with time because of traffic loading, environment conditions, and poor pavement maintenance management. The aim of this research is to implement close range photogrammetry technique for evaluation of the pavement surface distresses. The assessment was based on comparison with the traditional visual inspection method and validation of its equivalency with visual evaluation. The asphalt concrete pavement surface distresses such as (cracking type and crack width, patching area, rut depth and potholes area and depth) have been assessed. The visual inspection was conducted by walking through the roadway and evaluating the pavement surface distress visually. As for the photogrammetric fieldwork, it starts with generation of ground control points around the area of distress. A total station device (Topcon, GTS 235) was used to measure the coordinates (X, Y, and Z) for GCPs and the initial camera positions. The coordinates of two points (two base stations) referenced these coordinates. Within the study area, forty vertical stereo pair images of different pavement distresses were captured using a non-metric DSLR camera. Photogrammetric process was carried out by using ERDAS IMAGINE software Version 8.4 to create ortho-images and evaluate pavement surface distress. Window measurement tool in ortho-rectified image provides all the fundamental quantitative measurement functions necessary to measure length, area, width and other pavement distress condition. Results of the two techniques (photogrammetric and visual methods) were modeled. It was concluded that using photogrammetric approach is efficient in evaluating the pavement with a high (R^2) range between (0.985 and 0.999) as compared to the visual evaluation. Further, the photogrammetric technique could provide a permanent documentation of the pavement surface condition, which could be referred when needed.

Keywords: *Asphalt concrete, pavement, distress, visual assessment, close range photogrammetry*

****Author for Correspondence**: Email ID: saadisasarsam@coeng.uobaghdad.edu.iq*

INTRODUCTION

The evaluation of pavement surface condition is considered as a first step in scheduling the pavement maintenance program and assessment of budget requirements. Many techniques have been established for such process, such as GIS, video imaging with image processing software and even visual examination. Close range photogrammetry may be used as a research tool in civil engineering such as pavement evaluation monitoring. Little attention has been provided to the close range photogrammetry technique; this could be due to the fast development in instrumentation and testing procedures[1]. One of the most common methods of obtaining pavement distress information is by visual inspection of cracks and potholes that is performed by a walking rating technician according to certain specifications[2]. The principal method for crack survey is to use the manual technique and examine visual information collected in the field to determine the conditional parameters[3]. The most widely known and researched form of close-range digital photogrammetry is the stereo close-range digital photogrammetry. A digital close range photogrammetric technique allows converting images of an object into a 3D model. The photogrammetric 3D coordinate determination is based on the collinearity equation[4]. A sufficient number of control points must be recorded to adequately orient the image and transform the image coordinates into real world coordinates. ERDAS IMAGINE software[5] enables surface conditions to be represented as ortho-image. Close-range digital photogrammetry is seen as a possible approach in providing geometrical imaging for pavement distress studies without physically touching the surface being measured. The results obtained by this technique are compared with the traditional method of visual inspection[1]. Manual assessment can be finished directly on the road or later in the office[6].

The objective of this study was to investigate the potential capabilities and flexibility technique of the measurement-based vertical stereovision system and ERDAS IMAGINE 8.4 software in quantification of pavement distresses, the possibility of using digital close range photogrammetric approach in evaluating asphalt pavement surface distresses such as rutting depth, cracking type, crack width, patching condition, and potholes depth, may be detected based on the analysis of the captured vertical stereovision images using ERDAS IMAGINE 8.4 software. Comparison between the traditional visual technique and photogrammetric examination technique for obtaining pavement surface-distress condition, and evaluation of the suitability of the proposed techniques were detected in this work.

VISUAL OBSERVATION

Visual observation of pavement distress is the most common method for monitoring pavement surface condition. This has been traditionally performed by trained engineers who walk or drive along the road to assess the distresses and subsequently produce report sheets. Walking provides more detailed data than driving, but it is more dangerous and time-consuming[7]. In addition, the accuracy and consistency of the data also depend on the experience of the inspectors who perform the survey. However this method of field inspection poses several drawbacks, such as it is slow and labor intensive, it is inflexible and does not provide an absolute measure of the surface, moreover it could expose a serious safety hazard to the surveyors due to high speed and high volume traffic[8].

STEREO PHOTOGRAMMETRIC TECHNIQUES

A prominent part of the photogrammetric community’s effort has, for a long time, been the recovery of the three-dimensional description of the object space by stereoscopy. Stereo vision is a natural phenomenon that makes the overlapping area of two images, acquired from two different viewpoints by the same sensor; appear as one three dimensional scene if each photograph is viewed with one eye separately. Therefore, the missing depth information can be recovered[9]. Stereo imaging involves obtaining two view of the object of interest. The distance between the centers of the two camera lens locations is called the base line (in the close range). If an object point P appears in the scene, the objective is to find the object space coordinates (X, Y, Z) of the point, given its image point coordinates (xL, yL) on the left photograph and (xR, yR) on the right photograph, in addition to the camera parameters[9]. Image-collection technology is seemingly the most popular approach. Most systems record pavement surface images using a video camera or photographic camera mounted on a survey vehicle. Photogrammetric evaluation is either done manually by capturing image and specially designed workstations while trained crews rate the recorded road surface or automatically by computer image processing software[10].

In the present study, a frame was designed to handle the digital camera into two exposure stations; such a frame could be fixed on a tripod. That camera is directed in a perpendicular position on the roadway at a certain station. Then, the set with the camera is transported to other spot within the area. Figure 1 shows the designed frame. This frame was designed by fixing the height of photo exposure to 1 m, the desired focal length is 24 mm, photo overlapping 60% as shown in Figure 2, therefore, the base line become 37.5 cm, while Figure 3 shows the non-metric DSLR camera (Canon EOS 600D) implemented in the work.

Fig. 1: *The Designed Frame*

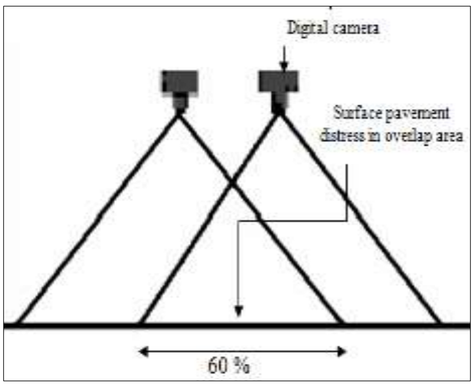

Fig. 2: *Stereo Image Overlap.*

Fig. 3: *Canon EOS 600D Camera.*

Photogrammetric fieldwork began with creation of certain distribution of control points around the area of distress. Ground control points are necessary for photo triangulation computations. At least three ground control points (GCPs) spread across each image were marked and measured with a total station device (TOPCON, GTS 235) shown in Figure 4. On the other hand, Figure 5 shows differential global position system (DGPS) device. GCPs were referenced by to the tow points measured by using differential global position system (TOPCON Hipper-GR3).

Fig. 4: *Total Station Device.*

Fig. 5: *DGPS Device.*

METHODOLOGY OF CLOSE RANGE PHOTOGRAMMETRY

Close range photogrammetry is used to refer to photographs with an object-to camera distance of less than 300 m[11]. The goal is to develop a working system that is able to establish three-dimensional (3D) surface model of pavements with image processing system.

Two digital cameras are used to cover half of a lane-width, approximately 2 m. The pair of images on the same pavement surface is also used to establish 3D surface model, which is then used to detect the deficiencies of the pavement surface condition. Pavement condition survey includes surface distresses, such as cracking, roughness and rutting, and other surface defects.

At least three ground control points (3GCPs) were recognized and matched to enable relative orientation and stereo-model generation. Figure 6 shows the tilted images obtained from two overlapping images, while Figure 7 shows that the tilted images are transformed to normalized images. Triangulation was performed by Ortho BASE project in ERDAS IMAGINE software to estimate the (X, Y, Z) locations of tie points in stereo model, and the exterior orientation parameters (EOP) of images can be computed. The distribution of the ground control points, and other points in the adjusted stereo model was shown in Figure 8. Generally 3GCPs in overlap area must be identified in each image of stereo pair and several tie points are additional points were measured on stereo image. After performing triangulation with ERDAS IMAGINE software, ortho-images were created. Window measurement tool in ortho rectified image provides all the fundamental quantitative measurement functions of each single stereo model that is necessary to measure width, lengths, area and other distress condition.

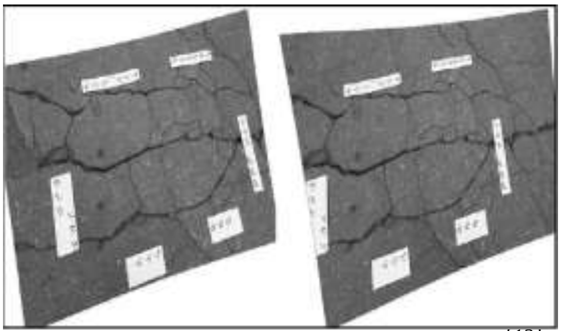

Fig. 6: *Two Overlapping Tilted Image[12].*

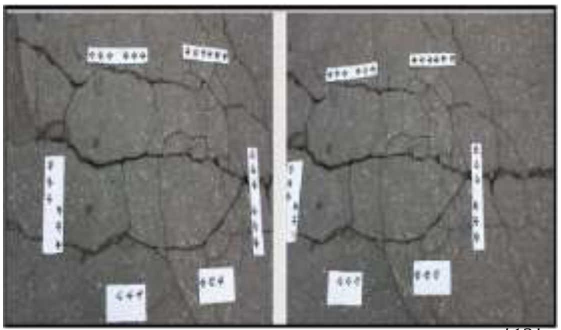

Fig. 7: *Generated Normalized Images[12].*

Digital Image

A digital image is a computer-compatible pictorial rendition in which the image is divided into a fine grid of picture elements or pixels. The image consists of an array of integers, often referred to as digital numbers, each quantifying the gray level, or degree of darkness, at particular elements[13].

The digital image may consist of as many thousands or millions of these pixels appearing to be that of a continuous tone picture. Each pixel represented by a value from 0 (dark black) to 255 (bright white), the range of values (0 to 255) can be explained by examining how computers deal with numbers. Since computers operate directly in binary number system, it is most efficient to use ranges corresponding to powers of 2. Photogrammetric techniques allow converting images of an object into a 3D model by using a digital camera. The photogrammetric 3D coordinate determination is based on the collinearity equation.

Processing Digital Imagery and Ortho BASE Triangulation

Digital imageries were entered directly into softcopy photogrammetric software after images were captured. The software uses a technique known as bundle block adjustment for triangulation which establishing a mathematical relationship between the images contained in a project, the camera, and the ground[5]. The internal geometry of each image and the relationships between overlapping images are determined. At least three ground control points in overlap area are fixed to transform the image coordinates into real world coordinates. These points are clearly visible on the photographic image as shown in Figure 8.

The orientation serves to relate the overlapping portions of left and right images to create the stereo model. After performing relative orientation; the images were then displayed simultaneously to allow generated common points to be identifiable on the stereo overlap for each image. This enabled the overlapping portions of both image to be merged together to provide a 3D stereo image, absolute orientation was the final orientation process carried out to tie the 3D stereo image into a real world coordinates system as directed by Kim[14].

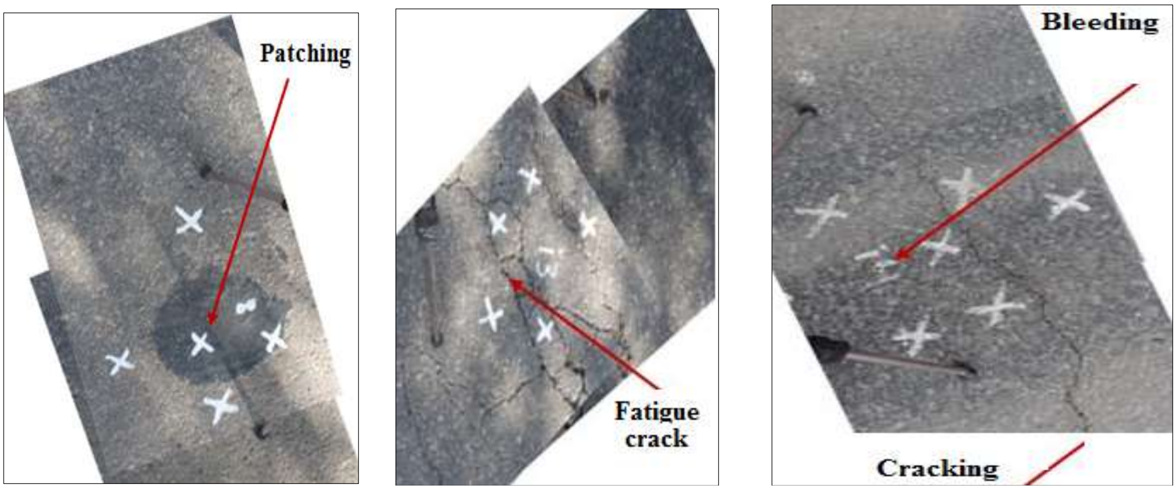

Fig. 8: *Ortho-Rectified Image Showing Ground Control Points.*

Collinearity Equations

The fundamental geometric relationship between object space and image coordinates is called collinearity equations (Figure 9). Collinearity assumes that object point A (XA, YA, ZA), perspective center P (XO, YO, ZO) and image point a (xa, ya) lie on the same line. Control points were represented with the small targets with known coordinates (X, Y, Z) measured in the field. Then, stereo-images collected at specific locations were recorded as shown in Figure 10.

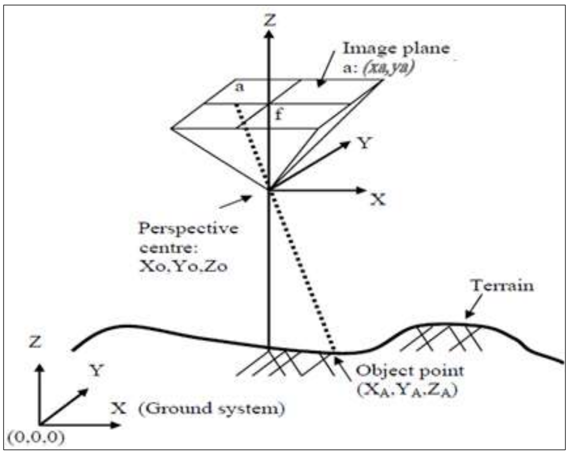

Fig. 9: *Relationship between Images Coordinate and Object Space[9].*

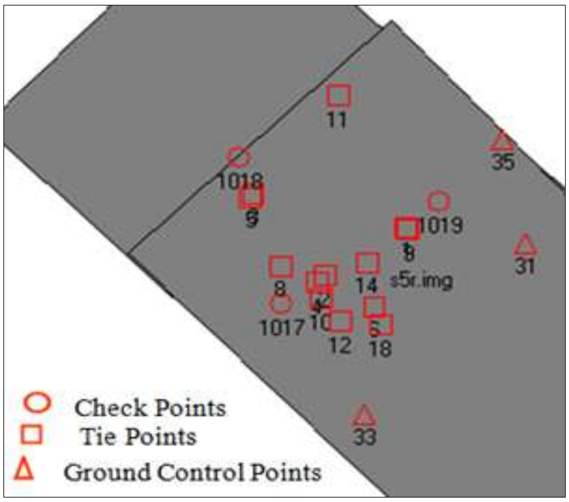

Fig. 10: *Distribution of Ground Control Points, Tie Points and Check Points in the Adjusted Stereo Model.*

ASSESSMENT OF ASPHALT CONCRETE PAVEMENT DISTRESSES

Fatigue Cracking

Table 1 shows the assessment of fatigue crack area, width and intensity using (photogrammetric and visual methods). Figure 11 shows the results obtained by using both methods, it shows high correlation as indicated by high coefficient of determination R^2 = (0.999), (0.996), (0.999) for area, width and intensity respectively. The defected area with fatigue cracks is higher when using close range photogrammetry as compared to that of visual technique as indicated by 45° line.

Table 1: *Fatigue Cracking Assessment Using Visual and Photogrammetry Techniques.*

Section		**Fatigue - Crack Sample ID**	**Area (m^2)**		**Width (mm)**		**Intensity (%)**	
From	**To**		**Visual Technique**	**Photo Technique**	**Visual Technique**	**Photo Technique**	**Visual Technique**	**Photo Technique**
0+150	0+200	3	0.87	0. 85	20.0	20.7	0.22	0.26
0+500	0+550	19	0.61	0.45	3.0	2.85	0.65	1.17
		22	2.10	1.87	3.5	3.26		
0+700	0+750	25	15.0	14.69	4.0	3.92	8.08	8.23
		80	10.5	10.35	13.0	12.85		
1+300	1+350	2534	3.31	3.08	86.0	84.4	14.73	15.09
		38	48.0	47.02	20.0	20.04		
2+150	2+200	55	3.49	3.30	75.0	77.0	13.54	13.79
		56	42.0	41.39	25.0	22.6		
		57	1.41	1.34	20.0	20.7		
Regression model			Y= 0.099 + 1.015 X		Y = 0.200 + 0.997 X		Y = 0.245 + 1.002 X	
Coefficient of determination R^2			0.999		0.996		0.999	

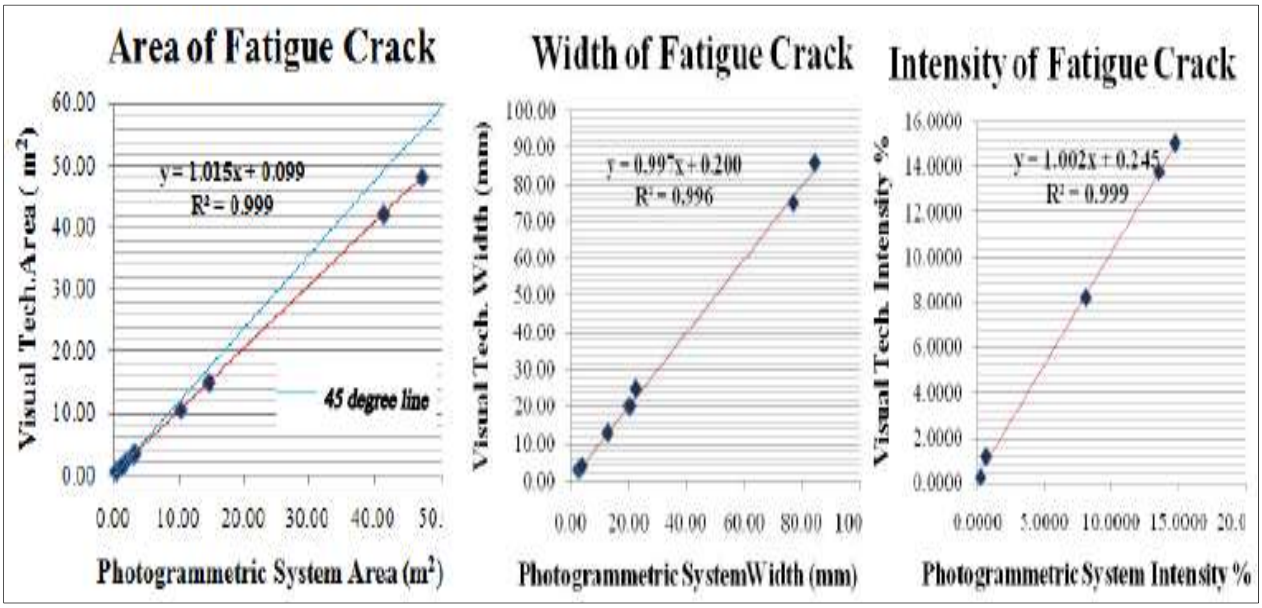

Fig. 11: *Fatigue Cracking Variables Assessed by Both Techniques.*

Block Cracking

Table 2 shows the assessment of block cracking area, width and intensity using both testing methods (photogrammetric and visual methods). Figure 10 shows the results obtained by using both methods, it shows high correlation as indicated by high coefficient of determination R^2=(0.995), (0.997), (0.999) for area, width and intensity respectively. The width of block cracking width is higher when visual technique is implemented as indicated by 45° line. This agrees well with Kertész *et al.*[15].

Table 2: *Block Cracking Assessment Using Visual and Photogrammetry Techniques.*

Section		Block - Crack Sample ID	Area (m^2)		Width (mm)		Intensity (%)	
From	**To**		**Visual Technique**	**Photo Technique**	**Visual Technique**	**Photo Technique**	**Visual Technique**	**Photo Technique**
0+700	0+750 a	24	20.0	19.63	4.0	4.25	14.97	14.69
	b	26	26.4	25.92	100.0	98.1		
0+250	0+300	84	13.19	12.17	40.0	41.34	3.86	3.56
2+150	2+200	72	18.13	16.64	15.0	14.74	5.33	4.90
Regression model			Y = 1.864 + 0.944 X		Y = 0.687 + 1.021 X		Y = 0.393 + 0.992 X	
Coefficient of determination R^2			0.995		0.997		0.999	

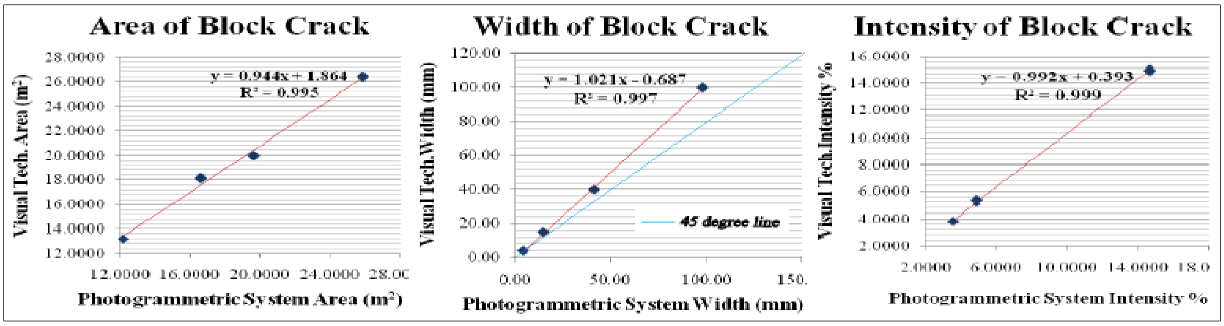

Fig. 12: *Block Cracking Variables Assessed by Both Techniques.*

Longitudinal Cracking

Table 3 shows the assessment of longitudinal crack length, width, and intensity using both testing methods (photogrammetric and visual methods). Figure 13 shows the results obtained by using both methods, it shows high correlation as indicated by high coefficient of determination R^2 = (0.999), (0.996), (0.999) for length, width, and intensity respectively. The longitudinal cracking intensity is higher when visual technique is implemented as indicated by 45° line.

Table 3. *Longitudinal Cracking Assessment Using Visual and Photogrammetry Techniques*

Section		Longitudinal Crack Sample ID	Area (m^2)		Width (mm)		Intensity (%)	
From	**To**		**Visual Technique**	**Photo Technique**	**Visual Technique**	**Photo Technique**	**Visual Technique**	**Photo Technique**
0+500	0+550	19	7.3	7.27	16.0	16.40	34.68	33.93
	a	22	7.0	6.92	18.0	16.93		
	b c	23	2.8	2.78	30.0	29.00		
2+250	2+300	66	3.8	3.78	22.0	22.28	28.36	28.21
2+600	2+650	71	2.6	2.59	6.00	5.48	5.80	5.18
Regression model			Y = 0.009 + 1.009 X		Y = 0.223 + 1.008 X		Y = 0.561 + 0.997 X	
Coefficient of determination R^2			0.999		0.996		0.999	

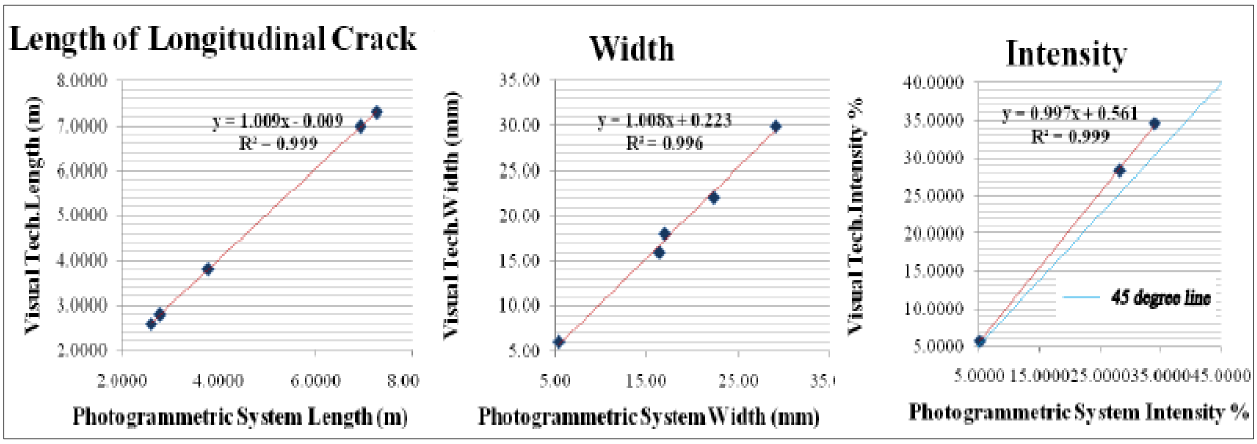

Fig. 13: *Longitudinal Cracking Variables Assessed by Both Techniques.*

Transverse Cracking

Table 4 shows the assessment of crack area, width, and intensity using both testing methods (photogrammetric and visual methods). Figure 14 shows the results obtained by using both methods, it shows high correlation as indicated by high coefficient of determination R^2=(0.999), (0.998), (0.998) for area, width and intensity respectively. The transverse crack width is higher at visual technique when compared to photogrammetry technique as indicated by 45° line.

Table 4: *Transverse Cracking Assessment Using Visual and Photogrammetry Techniques.*

Section		Transverse Crack Sample ID	Area (m^2)		Width (mm)		Intensity (%)	
From	**To**		**Visual Technique**	**Photo Technique**	**Visual Technique**	**Photo Technique**	**Visual Technique**	**Photo Technique**
0+150	0+200 a	3	21.98	21.06	7.0	6.53	7.83	7.13
	b	5	3.0	2.91	1.0	1.18		
0+250	0+300	9	2.49	2.45	15.0	16.20	0.741	0.730
1+300	1+350a	78	6.34	6.25	25.0	26.51	14.16	14.03
	b	39	41.80	41.44	40.0	40.90		
Regression model			Y = 0.132 + 1.011 X		Y = 0.073 + 0.967 X		Y = 0.225 + 1.007 X	
Coefficient of determination R^2			0.999		0.998		0.998	

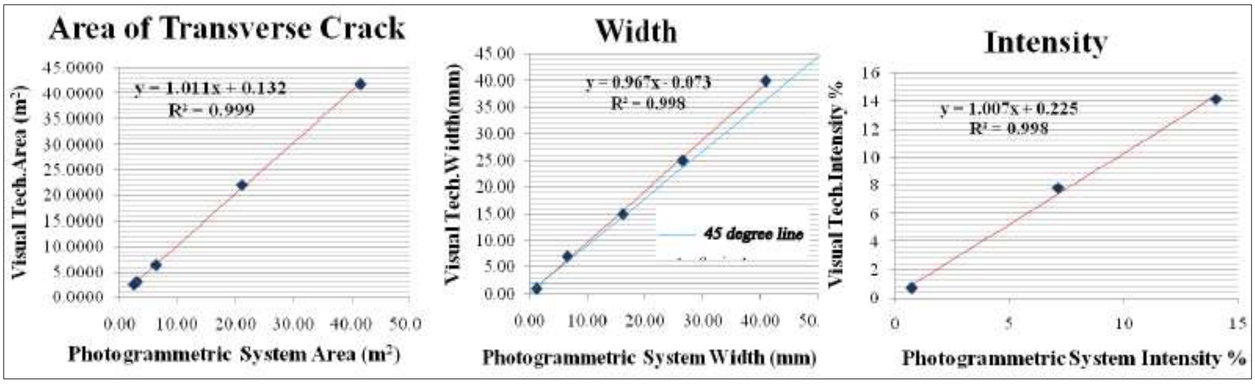

Fig. 14: *Transverse Cracking Variables Assessed by Both Techniques.*

Edge Cracking

Table 5 shows the assessment of edge cracking width and intensity using both testing methods (photogrammetric and visual methods). Figure 15 shows the results obtained by using both methods, it shows high correlation as indicated by high coefficient of determination R^2 = (0.994), and (0.999) for width and intensity respectively. The edge crack width is higher when using visual technique as indicated by 45° line.

Table 5: *Edge Cracking Assessment Using Visual and Photogrammetry Techniques.*

Section		Edge Crack Sample ID	Width (mm)		Intensity (%)	
From	**To**		**Visual Technique**	**Photo Technique**	**Visual Technique**	**Photo Technique**
0+050	0+100	2	15.0	13.69	24.96	24.52
	a b	21	17.0	16.36		
0+4250	0+300	9	5.00	4.98	14.66	14.30
2+700	2+750	73	15.0	14.4	5.26	5.43
Regression model			Y = –0.232 + 1.070 X		Y = –0.251 + 1.031 X	
Coefficient of determination R^2			0.994		0.999	

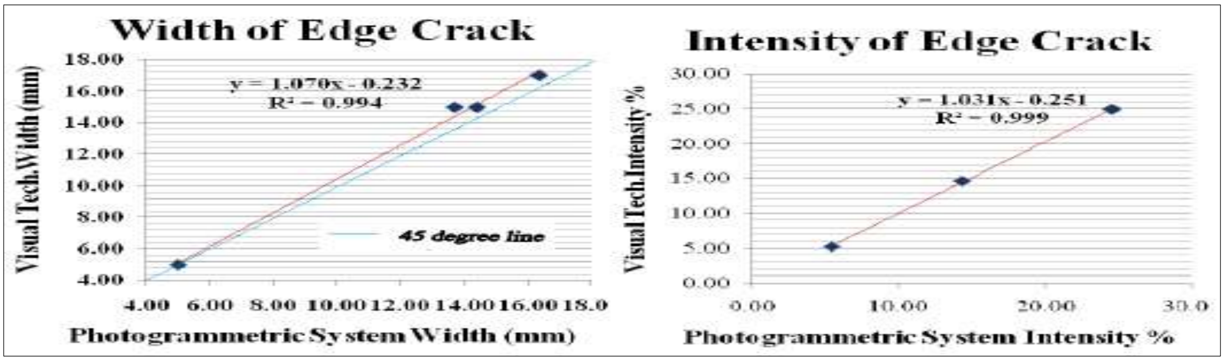

Fig. 15: *Edge Cracking Variables Assessed by Both Techniques.*

Rutting

Table 6 shows the assessment of rutting area, depth and intensity using (photogrammetric and visual methods). Figure 16 shows the results obtained by using both methods, it shows high correlation as indicated by high coefficient of determination R^2 = (0.997), (0.985), (0.996) for area, depth and intensity respectively. The defected area by rutting is higher when using visual technique as indicated by 45° line. Similar findings were reported by Grondin *et al.*[16].

Table 6: *Rutting Assessment Using Visual and Photogrammetry Techniques.*

Section		Rutting Sample ID	Area (m^2)		Depth (mm)		Intensity (%)	
From	**To**		**Visual Technique**	**Photo Technique**	**Visual Technique**	**Photo Technique**	**Visual Technique**	**Photo Technique**
1+250	1+300	33	4.20	4.16	2.0	2.14	1.24	1.22
1+300	1+350	34	3.31	3.08	4.0	4.12	1.23	1.16
		38	0.88	0.85	4.0	4.17		
2+150	2+200	57	3.10	2.95	5.0	5.29	1.67	1.61
		59	1.60	1.57	5.0	5.09		
		60	0.97	0.96	4.0	4.26		
2+250	2+300	64	4.68	4.60	5.0	5.20	2.27	2.15
		65	2.10	1.94	7.5	7.20		
		67	8.40	7.86	4.0	4.67		
Regression model			Y = –0.049 + 1.060 X		Y = –0.528 + 1.074 X		Y = –0.038 + 1.067 X	
Coefficient of determination R^2			0.9997		0.985		0.996	

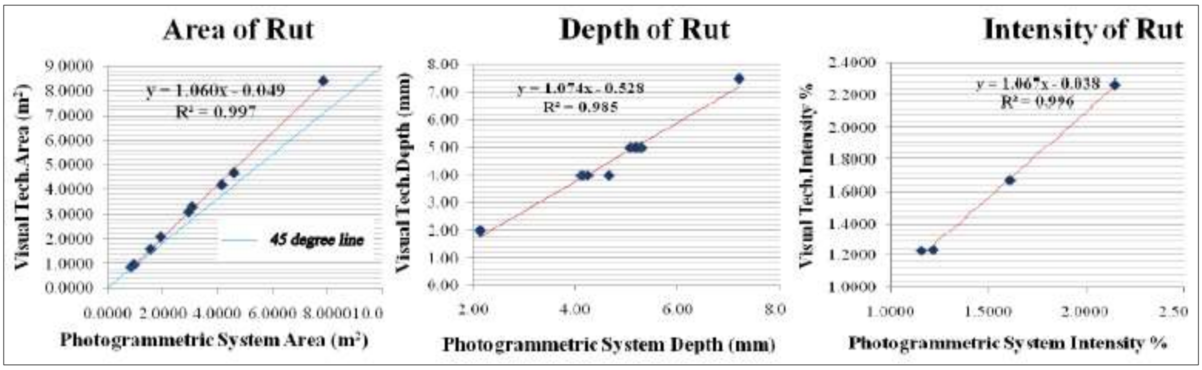

Fig. 16: *Rut Depth Variables Assessed by Both Techniques.*

Bleeding

Table 7 shows the assessment of bleeding area, and intensity using both testing methods (photogrammetric and visual methods). Figure 17 shows the results obtained by using both methods, it shows high correlation as indicated by high coefficient of determination R^2 = (0.999), (0.999) for area, and intensity respectively. The variation in the defected area with bleeding is not significant among both techniques as indicated by 45° line.

Table 7: *Rutting Assessment Using Visual and Photogrammetry Techniques.*

Section		Asphalt Bleeding Sample ID	Area (m²)		Intensity (%)	
From	To		Visual Technique	Photo Technique	Visual Technique	Photo Technique
0+050	0+100	1	12.76	12.42	3.80	3.70
0+150	0+200 a	4	5.78	5.59	4.97	4.60
	b	5	8.20	8.17		
	c	10	1.73	1.68		
2+250	2+300a	64	20.68	19.99	12.62	12.34
	b	67	63.90	62.70		
Regression model			Y = 0.062 + 1.019 X		Y = –0.199 + 1.007 X	
Coefficient of determination R^2			0.999		0.999	

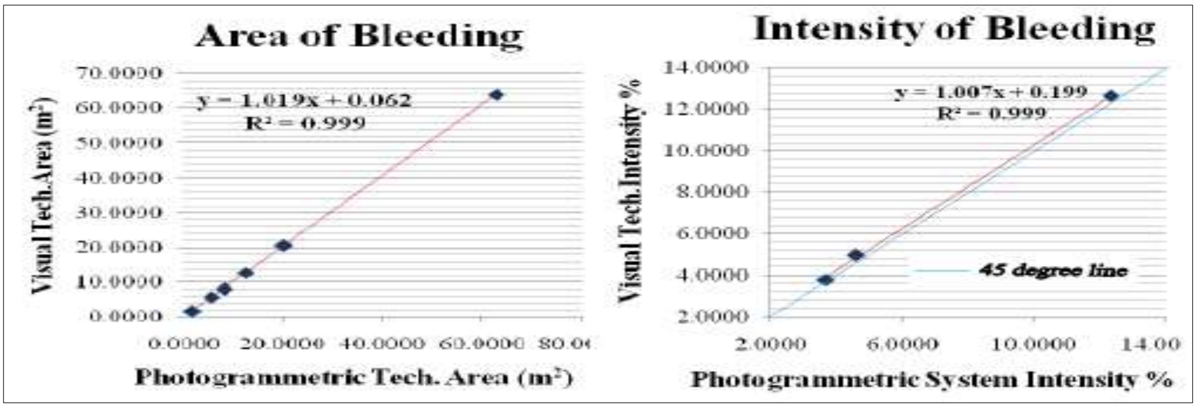

Fig. 17: *Asphalt Bleeding Variables Assessed by Both Techniques.*

Patching

Table 8 shows the assessment of patching area, and intensity using both testing methods (photogrammetric and visual methods). Figure 18 shows the results obtained by using both methods, it shows high correlation as indicated by high coefficient of determination R^2 = (0.998), (0.999) for area, and intensity respectively. The variation in the patching area is not significant among both techniques as indicated by 45° line. All of the distresses identified are in accordance to USDOT-FHA[17].

Table 8: *Patching Assessment Using Visual and Photogrammetry Techniques.*

Section		**Patching Sample ID.**	**Area (m^2)**		**Intensity (%)**	
From	**To**		**Visual Technique**	**Photo Technique**	**Visual Technique**	**Photo Technique**
0+250	0+300	77	0.2967	0.2953	0.0956	0.0352
2+150	2+200 a	59	7.3960	6.9669	4.4212	4.2756
	b	60	7.6360	7.5700		
2+700	2+750	74	0.0899	0.0933	0.029	0.0269
Regression model			Y = 1.032 X		Y = 0.030 + 1.027 X	
Coefficient of determination R^2			0.998		0.999	

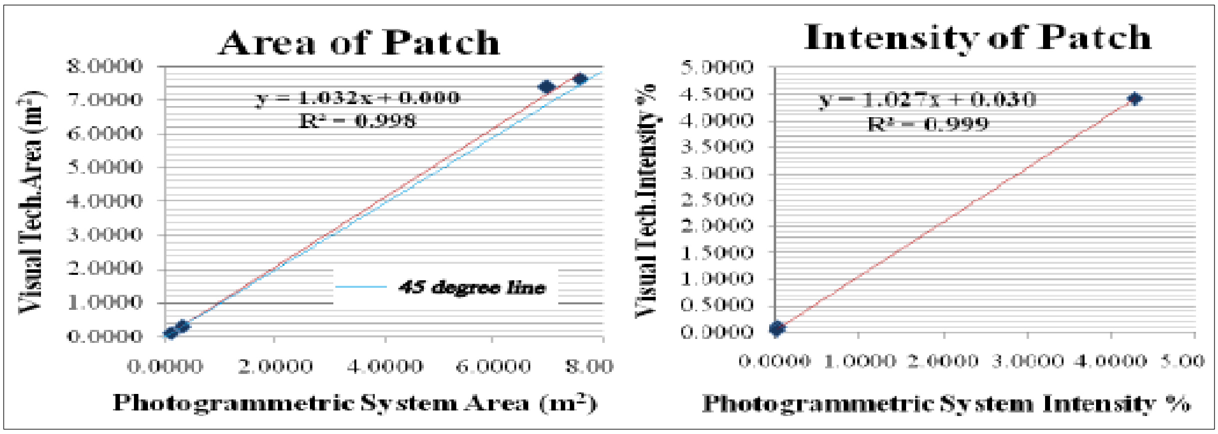

Fig. 18: *Asphalt Concrete Patching Variables Assessed by Both Techniques.*

Pothole

Table 9 shows the assessment of pothole area, depth and intensity using both testing methods (photogrammetric and visual methods). Figure 19 shows the results obtained by using both methods, it shows high correlation as indicated by high coefficient of determination R^2 = (0.999), (0.991), (0.998) for area, depth and intensity respectively. The depth of pothole is higher when measured by visual technique when compared with that by photogrammetry as indicated by 45° line.

Table 9: *Pothole Assessment Using Visual and Photogrammetry Techniques.*

Section		**Pothole Sample ID**	**Area (m^2)**		**Depth (mm)**		**Intensity (%)**	
From	**To**		**Visual Technique**	**Photo Technique**	**Visual Technique**	**Photo Technique**	**Visual Technique**	**Photo Technique**
0+250	0+300	8	0.0048	0.0049	4.00	5.13	0.0014	0.0015
1+300	0+350	35	0.3400	0.3377	40.0	39.9	0.1000	0.0993
1+750	1+800	48	0.0740	0.0791	30.0	32.0	0.1321	0.1037
	a	51	0.1037	0.1064	15.0	17.3		
	b	81	0.1794	0.1737	21.0	23.3		
	c							
2+150	2+200	55	0.0368	0.0304	5.00	4.50	1.0806	1.0582
	a	56	3.4500	3.3868	28.0	30.0		
	b	58	0.1872	0.1808	20.0	20.1		
	c							
2+600	2+650	70	0.0063	0.0075	25.0	26.7	0.0018	0.0022
Regression model			Y = 1.018 X		Y = –0.763 + 0.978 X		Y = 0.006 + 1.016 X	
Coefficient of determination R^2			0.999		0.991		0.998	

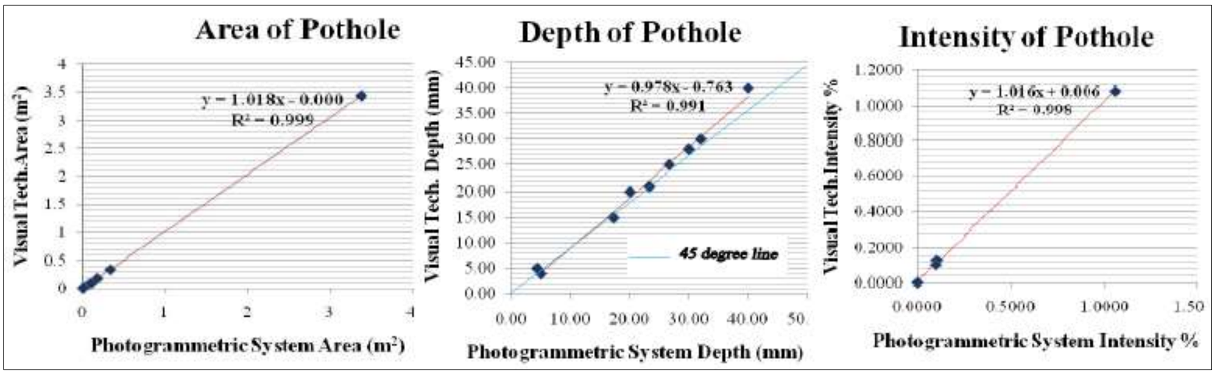

Fig. 19: *Pothole Variables Assessed by Both Techniques.*

Polished Aggregate

Table 10 shows the assessment of polished aggregate area, depth and intensity using both testing methods (photogrammetric and visual methods). Figure 20 shows the results obtained by using both methods, it shows high correlation as indicated by high coefficient of determination R^2 = (0.996), (0.988), (0.992) for area, depth and intensity respectively. The variation in the depth of area defected by polishing is significantly high when visual technique is used as indicated by 45° line.

Table 10: *Polished Aggregates Assessment Using Visual and Photogrammetry Techniques.*

Section		Polished Sample ID	Area (m²)		Depth (mm)		Intensity (%)	
From	**To**		**Visual Technique**	**Photo Technique**	**Visual Technique**	**Photo Technique**	**Visual Technique**	**Photo Technique**
1+250	1+300	33	4.20	4.16	1.09	0.93	1.24	1.22
1+300	1+350	34	3.31	3.08	1.16	0.96	4.44	4.02
	a b	35	10.65	10.58	1.35	1.22		
1+350	1+400	42	8.58	8.80	0.99	0.84	2.35	2.49
Regression model			Y = 0.168 + 1.005 X		Y = 0.242 + 0.919 X		Y = –0.297 + 1.153 X	
Coefficient of determination R^2			0.996		0.988		0.992	

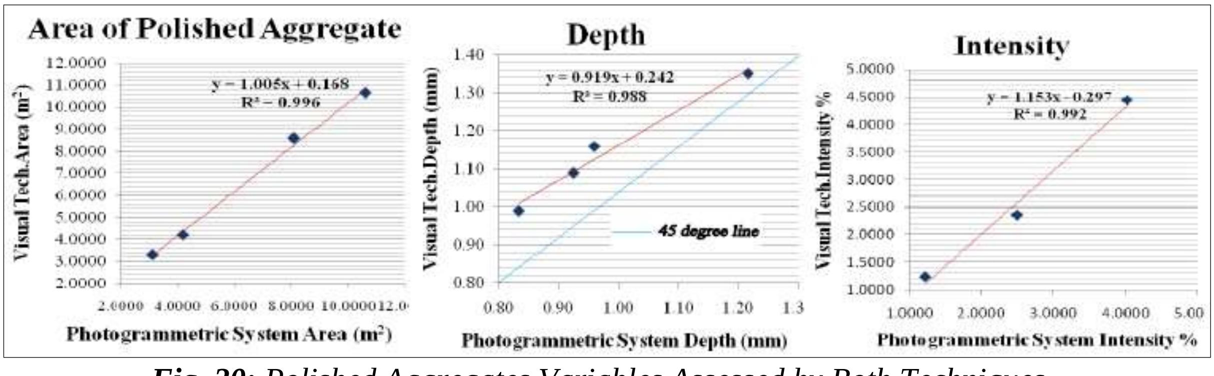

Fig. 20: *Polished Aggregates Variables Assessed by Both Techniques.*

Raveling

Table 11 shows the assessment of raveling area, depth, and intensity using both testing methods (photogrammetric and visual methods). Figure 21 shows the results obtained by using both methods, it shows high correlation as indicated by high coefficient of determination R^2 = (0.999), (0.990), (0.999) for area, depth and intensity respectively. The variation in pavement depth at the area defected with raveling is significant when using the visual technique as indicated by 45° line.

Table 11: *Pavement Raveling Assessment Using Visual and Photogrammetry Techniques.*

Section		**Raveling Sample ID**	**Area (m^2)**		**Depth (mm)**		**Intensity (%)**	
From	To		**Visual Technique**	**Photo Technique**	**Visual Technique**	**Photo Technique**	**Visual Technique**	**Photo Technique**
1+750	1+800	52	16.27	16.09	1.40	1.47	4.72	4.64
1+800	1+850	53	1.95	1.86	2.00	1.95	0.86	0.54
1+850	1+900	54	22.40	22.24	1.62	1.57	6.69	6.64
Regression model			Y = 0.092 + 1.003 X		Y = –0.159 + 1.109 X		Y = 0.338 + 0.951 X	
Coefficient of determination R^2			0.999		0.990		0.999	

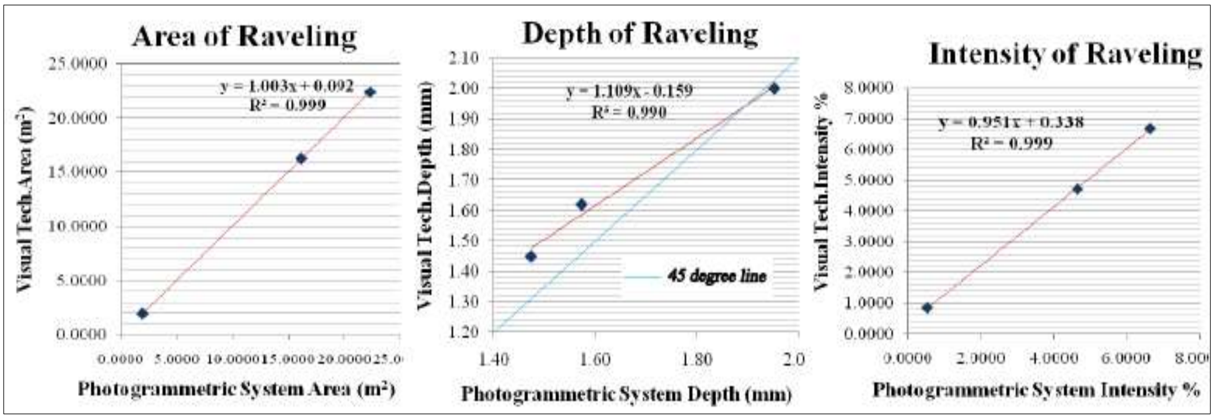

Fig. 21: *Pavement Raveling Variables Assessed by Both Techniques.*

CONCLUSIONS

Based on the limited field testing of asphalt concrete pavement surface distresses, the following conclusions may be drawn.

1. Photogrammetric approach is efficient in evaluating the Asphalt concrete with a high coefficient of determination ranged between 0.985 and 0.999 as compared to the traditional method of visual evaluation. The photogrammetric technique could provide a permanent documentation of the pavement surface condition, which could be referred when needed.
2. The defected area with fatigue cracks is higher when using close range photogrammetry as compared to that of visual technique, while the width of block cracking width is higher when visual technique is implemented.
3. The defected area by rutting is higher when using visual technique, while the variation in the defected area with bleeding or patching is not significant among both techniques.
4. The variation in the depth of area defected by polishing of aggregate or raveling is significantly high when visual technique is used.

REFERENCES

1. Chai L.T. *Evaluation of Cracks and Disintegration Using Close Range Digital Photogrammetry and Image Processing Technique*. M.Sc. Thesis, Department of Civil Engineering, College of Engineering, University Technology Malaysia. Apr 2005.
2. Miraz A., Gunaratne M., Nazef A., *et al. Experimental Evaluation of a Pavement Imaging System.* Florida Department of Transportation’s Multipurpose Survey Vehicle. TRB, Transportation Research Record: No. 1974, Washington, D.C. 2006; 97–106p.
3. Wang K., Gong W. Automated Pavement Distress Survey. A Review and a New Direction. *Pavement Evaluation Conference*, Virginia. 2002. http://Pms.Nevadadot.Com/2002/43.

4. Yakar M. *Data Collecting to Volume Computing Using Digital Close Range Photogrammetry and Laser Techniques*. At http://www.fig.net/pub/fig2008 /papers/ts02d-05-yakar-etal-3064.
5. ERDAS. Inc. *IMAGINE Ortho BASE User's Guide*, ERDAS IMAGINE V8.4, Atlanta, Georgia. 2003.
6. Sokolic I. *Criteria to Evaluate the Quality of Pavement Camera Systems in Automated Evaluation Vehicles*. University of South Florida, USA, 2003.
7. Sarsam S.I. Development of Asphalt Concrete Pavement Maintenance Management System Using Visual Evaluation of Pavement Surface Condition and Expert System. *Proceeding, 7th International Conference on managing Pavement Assets (ICOWEFAL),* Calgary, Alberta, Canada. Jun 2008.
8. Schmidt C., Shuler S. *Performance Evaluation of Various HMA Rehabilitation Strategies*. Colorado Department of Transportation, DTD Applied Research and Innovation Branch Report No. CDOT-2008-9.
9. Mikhail E.M., Bethel J.S., McGlone J.C. *Introduction to Modern Photogrammetry*. New York: John Wiley & Son, Inc., USA. 2001.
10. ACSIRO, Australia´s Commonwealth Scientific and Industrial Research Organization. *Automated Detection of Road Cracks.* http://www.csiro.au/solutions/psaa.html. Jun 15, 2009.
11. Matthews N.A. *Aerial and Close-Range Photogrammetric Technology: Providing Resource Documentation, Interpretation, and Preservation*. Technical Note 428, Sep 2008. USA.
12. Ahmed M.F.M, Haas C.T. The Potential of Low Cost Close Range Photogrammetry towards Unified Automatic Pavement Distress Surveying. *Proceedings of the Annual Waterloo Demographic Center Conference*. 2010.
13. Wolf R., Dewitt A. *Elements of Photogrammetry with Application in GIS*. 3rd Edn. Boston: McGraw-Hill, USA. 2000.
14. Kim S.H. Close Range Digital Photogrammetry in Civil Engineering. *ACI Structural Journal*. 2010; 12(2). Spain.
15. Kertész I., Lovas T., Barsi A. *Photogrammetric Pavement Detection System*. Jun 15, 2009. http://www.Isprs.Org/Congresses/ Proceedings/5_Pdf/156.Pdf.
16. Grondin M., Leroux D., Laurent J. *Advanced 3D Technology for Rut Measurements: Apparatus on Board of the Quebec Ministry of Transportation Multifunction Vehicle*. 2002. http://Pms.Nevadadot.Com /2002 presentations/40.Pdf. Accessed Jun 15, 2009.
17. USDOT-FHA. *Distress Identification Manual for the Long Term Pavement Performance Program.* FHWA-RD-03-031, US Department of Transport.

